TASK QUARTERLY 12 No 3, 197–207

STEADY AND UNSTEADY SIMULATION OF FLOW STRUCTURE OF TWO SURFACE-MOUNTED SQUARE QBSTACLES

MARCIN HUPTAS AND WITOLD ELSNER

Institute of Thermal Machinery, Częstochowa University of Technology,
Al. Armii Krajowej 21, 42-200 Częstochowa, Poland
{*huptas, welsner*}*@imc.pcz.czest.pl*

(Received 28 May 2008)

Abstract: The paper presents the numerical results obtained with the use of the FLUENT commercial code for analysing the flow structure around a single cube and two rectangular in-line surface-mounted bluff bodies immersed in a boundary layer. In the former case, clear effects of the inflow boundary layer thickness on the wall-shear stress within the wake of a single body are described. In the latter case, the grid resolution accuracy in predicting periodic vortex shedding from two tandem arrangement bodies is examined. Moreover, the aim of this study is to highlight the differences between steady and unsteady simulations.

Keywords: aerodynamics of surface-mounted objects, boundary layer flows

1. Introduction

Increased interest in the problem of bluff-body aerodynamics has been observed over the past few decades. It is governed by potential applications of the results in the design process of new buildings as well as optimization of the existing urban areas and city centers. The local wind climate influences the comfort around and between buildings, the life quality in urban areas as well as specific economical aspects of utilization of the defined zones.

The flow structure of a build environment is usually studied based on simplified configurations starting from single rectangular obstacles, where a horse-shoe vortex, which extends downstream along to the obstacle side. forms in the upstream separation zone. The flow separation from the obstacle walls results in strong shear layers along which the turbulence production is high. The resulting high turbulence level increases diffusion and enhances entrainment by a shear layer of a low momentum reverse flow in the near-wake which strongly affects the local pressure gradients and increases the mixing [1]. Another often investigated configuration are cubic obstacles in a tandem arrangement, where the flow field is further complicated by mutual interference. For that case, a small separation (intermittent), lock-on and large separation regimes similar to the two-dimensional geometries are observed which are strongly

affected by the influence of the ground vicinity [2]. The flow structure around surface-mounted obstacles depends on various factors. One of the most important factors is the oncoming boundary layer thickness δ related to the height of upstream obstacles H. For thin, laminar boundary layers, ($\delta/H < 0.3$) the structure of the upstream separation is characterized by a multiple secondary recirculation upstream of a horseshoe vortex [3]. For thicker, turbulent boundary layers ($\delta/H > 0.7$) the dynamic behavior of the pressure and velocity field is bimodal [4]. The subject of inlet boundary layer parameters will be discussed in detail in the next part of the paper. Other important factors are also the oncoming flow turbulence, the non-dimensional distance ratio (S/H) and the height ratio of the two consecutive bodies. The sheared flow effect caused by the atmosphere boundary layer modifies the flow pattern on the windward side of a high-rise block. Tall buildings, defined as those which protrude above their neighbors, act as scoops to collect the wind over much of their height and deflect it to the ground level. In front of a building exposed to the wind, a vortex forms below the stagnation point. This vortex is shed on each side of the building and it can produce excessively high winds at ground level, causing discomfort or ever danger.

The studies of the wind environment around buildings are generally performed as wind tunnel experiments since it is the most well-established way to simulate a natural wind. The alternative to the wind tunnel testing is the application of Computational Fluid Dynamics (CFD), which has been increasingly exploited in various ways recently. The usually applied method for computation of turbulent flows in wind engineering is the Reynolds Averaged Navier-Stokes (RANS) approach. Within this approach, the equations are averaged in time over all the turbulent scales, to directly yield a statistically steady solution of the flow variables. Another option is the use of standard turbulence models from the RANS approach in time-dependent simulations, which is normally called unsteady RANS (uRANS). However, the latter approach which should be applied when the flow is not statistically stationary, increases the computational expenses significantly. Turbulence modeling plays a crucial role in correctly predicting the complex behavior of such flows, however, it should be remembered that despite the time dependence, unsteady RANS is not a simulation of the turbulence but of its statistics only. To compare unsteady and steady RANS simulations, the results must be averaged over one period. The unsteady RANS is suitable for flows where the unsteadiness is determinable, *i.e.* the frequency spectrum shows a spike at a shedding frequency. This is the case of the flow around single and two surface-mounted cubes which is analyzed in the paper.

2. Computational details

A flow around a single cube and two rectangular in-line surface-mounted square cylinders immersed in a boundary layer is computed in this work. The geometries of the analyzed cases are sketched in Figure 1. Computations of a flow around a single obstacle have been carried out initially (Figure 1a). For that case an analysis of an inflow boundary layer has been performed. The continuous line shows the inlet profile of the thick boundary layer ($\delta/H = 2.353$) while the doted line depicts the inlet profile of the thin layer ($\delta/H = 0.1$). Figure 1b presents the configuration of two obstacles, where $H_1/H_2 = 0.6$ describes their height ratio and $S/B = 1.5$ the distance between

them. Three-dimensional steady and unsteady RANS simulations have been carried out using a commercial CFD code, FLUENT v.6.2, with the RNG version of a k-ε turbulence model. According to the literature [5, 6] this model is widely used for flows in a build environment. Using this model, Ferreira *et al.* [5] have found a good agreement between computation and measured the building interference effects on pedestrian level comfort. Also Richards *et al.* [6], having computed the pedestrian level wind speeds in Auckland, have obtained results which are similar to the wind tunnel erosion patterns.

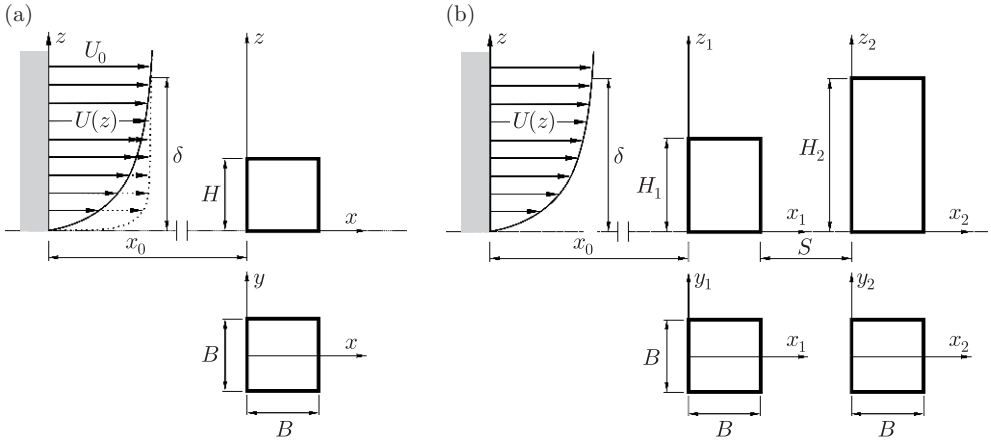

Figure 1. Scheme of considered flow: (a) single cube; (b) two tandem arrangement objects

The spatial derivatives have been discretized using a second order upwind scheme while the pressure-velocity coupling has been achieved using the SIMPLE algorithm. The unsteady calculations have been performed using normalized timestep $\Delta t^* = \Delta t \cdot U_0/B = 0.15$ where Δt is the timestep based on an estimation through experimental evidence and comprises 1% of the flow oscillations period.

The blockage ratio, defined as the ratio of the frontal area of the body to the computational domain cross-sectional area has been ≈ 0.7. For computation purposes, the flow domain is divided into a number of hexahedral cells. The mesh is nonuniform in all the three directions. The grid is clustered near the object and the spacing is increased to a proper ratio of 1.2 away from the object surface. The first cell adjacent to the walls has been set with respect to the criteria required for the individual near-wall treatment. Hence, using a two-layer approach, the width of the near-wall cell has been $0.003H$, which corresponds to $1 < y^+ < 3$ where H is the cube height. According to the literature [7] at least 10 cells per the cube root of the object volume should be used for a flow around surface-mounted obstacles. This recommendation given above has determined the initial minimum grid resolution which is $66 \times 70 \times 46$ per cube. The grid independent solution has been obtained for $135 \times 143 \times 94$ by systematically refining the entire mesh in each direction, increasing the number of nodes by about 50% [8]. The resolution for tandem arrangement objects has been set using the same methodology. The resolution for a coarse and fine (optimal) grid has been $114 \times 72 \times 50$ and $253 \times 143 \times 114$, respectively. Figure 2 shows the mesh used in the present simulations adequately for a single cube and dual objects configuration.

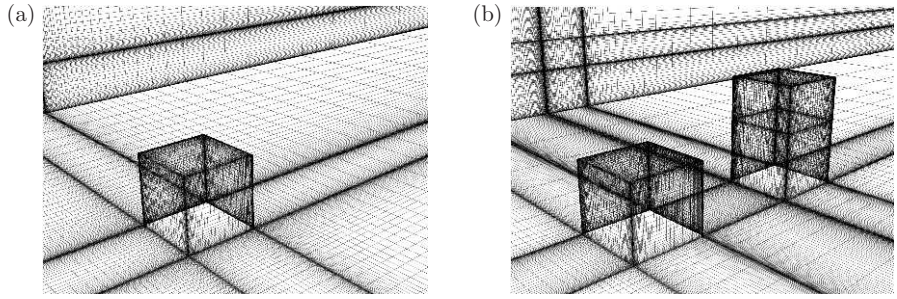

Figure 2. Computational mesh: (a) for single cube; (b) for tandem arrangement

3. Inlet boundary conditions

The inflow boundary layer has been prescribed according to [7] at a distance of $x_0 = 5H$, where H is the object height. For the second configuration, H has been replaced by $H_{\max}$ *i.e.*, the height of the tallest building. The oncoming flow profiles have been approximated using the power distribution $U(z) = U_\delta(z/\delta)^\alpha$, where α characterizes the terrain type. In addition to the inlet velocity profile, the k-ε RNG turbulence model requires an appropriate distribution of the turbulent kinetic energy k and the dissipation rate ε which together define the velocity and length scale of the turbulent motion. Different definitions of inlet boundary conditions have been analyzed and compared with experimental data [8]. One of the best methods to describe the inlet boundary conditions is the method proposed by Richards and Hoxey [9]. They define k and ε profiles as: $k = u_*^2/\sqrt{C_\mu}$ and $\varepsilon(z) = u_*^3/\kappa z$, where $C_\mu = 0.09$ and the von Karman constant $\kappa \approx 0.41$. For this study the friction velocity $u_* \approx 0.04U_0$, where U_0 is the free stream velocity, has been assumed after Bradshaw [10]. This, method has been accepted for the calculations described in the paper.

4. The role of inflow boundary layer thickness

As has been mentioned in the first chapter, the ratio of the incoming boundary layer thickness to the objects height δ/H has an important influence on the flow structure, and particularly, on the separation regions upstream and downstream the obstacle. As has been shown, for example, by Hunt *et al.* [11] and Castro and Robins [12], the shape and form of the separation region is markedly reduced by the presence of upstream nearwall turbulence.

To confirm these observations, steady simulations of a flow around a single cube immersed in a thin and thick boundary layer have been carried out. The thin boundary layer comprises 10% of the cube height ($\delta/H = 0.1$) while the thick layer – more than 230% ($\delta/H = 2.353$). The thick boundary layer is typical for a flat terrain characterized by the power exponent $\alpha = 0.195$. For both cases the Reynolds number $\mathrm{Re}_B = 27\ 000$ based on the free-stream velocity $U_0 = 13.5\,\mathrm{m/s}$ and the cube width $B = 0.034\,\mathrm{m}$.

The longitudinal wall shear stress (τ_x) distribution at the symmetric line ($y/B = 0$) in the wake for two flow cases compared to the experimental results (blue line) is presented in Figure 3. Wall shear stresses measurements in the wind

tunnel were made by the constant temperature anemometry with flush-mounted probe (CTA FM). The inlet conditions of the experiment were the same as those imposed at the inlet to the computational domain for $\delta/H = 2.353$. Separation and reattachment points could be easily recognized by the zero values of shear stresses. It can be observed that the size of the cavity region is significantly reduced in the presence of a thicker boundary layer. The maximum amplitude of shear stresses in the cavity zone range is also smaller. The difference is of the order of 30%. Evident overestimation of separation zone is noticed even for $\delta/H = 2.353$ when compared to the experimental data.

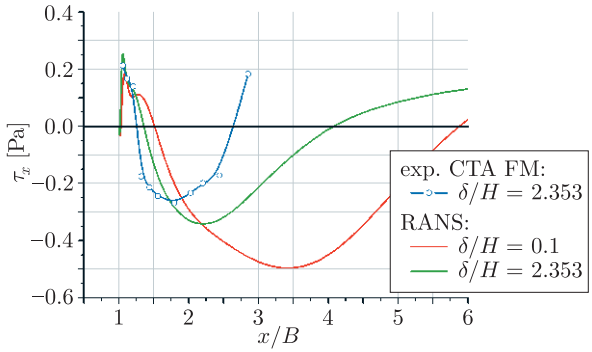

Figure 3. Comparison of experimental and numerical longitudinal wall shear stresses distribution at line $y/B = 0$ in the wake for flow around a single cube

It could be supposed that the reason for such an erroneously long separation is due to the fact that an important component of the flow field, *i.e.* the periodic vortex shedding, is omitted in steady calculations. A similar conclusion has been formulated by Iaccarino *et al.* [13] who show the difficulty in reproducing the main characteristics of the flow *i.e.* the recirculation length, backflow intensity and boundary layer recovery using the steady RANS models. The periodicity is a result of coupled oscillations between the separated shear layers from the lateral sides, which is similar to the vortex-shedding process for two-dimensional obstacles. However, for surface-mounted obstacles, this process is modified by the shear layer along the obstacle free-end (top), the oncoming flow shear gradient and horseshoe vortices. In that case, using the uRANS calculation should improve the agreement between the numerical and experimental prediction of the cavity zone. Apart from the quantitative disagreement with the experiment, the above results confirm the important role of the inlet boundary layer thickness on the flow structure around the obstacle.

5. Unsteady computation of single cube

Figure 4 gives a comparison of wall shear stresses distributions within the cube wake for the two considered cases obtained with the steady-state (RANS) and unsteady (uRANS) methods. Figure 4a presents the data taken along the central line $y/B = 0$ and Figure 4b along the line $y/B = 0.5$.

The analysis begins from the case of a cube immersed in a thin boundary layer $\delta/H = 0.1$(red lines). As can be noticed in Figure 4a, the size of the cavity zone is significantly smaller for the unsteady simulation (the time-average data) than for the

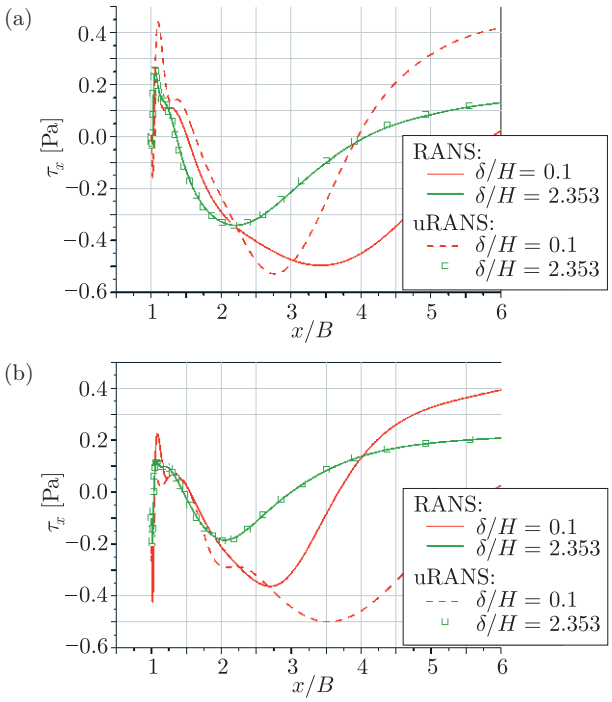

Figure 4. Distribution of longitudinal wall shear stresses in the wake for flow around a single cube for a steady and unsteady simulation: (a) on the ground at the symmetric line $y/B = 0$; (b) and at the line $y/B = 0.5$

steady calculation and closer to the experimental results. It means that the choice between RANS and uRANS is of high importance in that case. The above could be confirmed looking on the visualisation of wall shear stresses at the line $y/B = 0.5$ (Figure 4b).

The time evolution of wall shear stresses on the ground over one period is reported in Figure 5. The flow is evidently periodic, showing side-to-side oscillations. The regular passage of large-scale coherent structures *i.e.* vortices, responsible for the periodicity is observed in Figure 6 where the time history of the static pressure on the floor is observed. Vortex shedding from the cube lateral sides is correlated with low pressure regions. These vortices are a part of a big vertical structure called an arch-vortex detected in the wake of each surface-mounted object. The eddies are convected downstream and disappear at the distance equal to doubled height of the cube. It means that oscillatory unsteadiness is confined only to the rear wall of the cube, so the phenomenon cannot be directly associated with a two-dimensional von Karman street.

A similar numerical analysis of the flow around a single cube immersed in a thin boundary layer ($\delta/H = 0.07$) has been also performed by Iaccarino [13]. They have applied the $v^2 - f$ turbulence model for three-dimensional steady and unsteady RANS simulations. Their skin-friction results on the ground obtained with unsteady calculations give a better match with the experimental data than those form steady calculations. Even so, they produce an almost 20% longer separation zone than that observed for the oil-film flow visualization reported by Martinuzzi and Tropea [1]. It

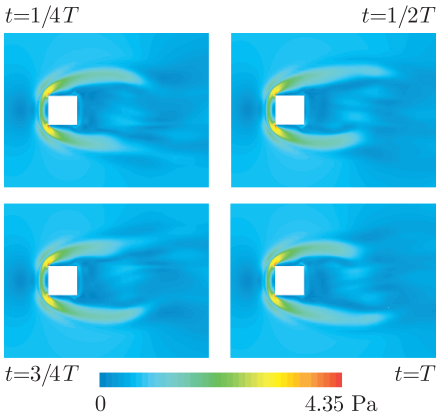

Figure 5. History of the wall shear stresses distribution on the ground

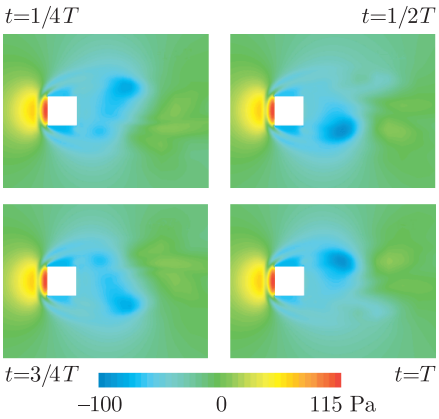

Figure 6. History of the pressure distribution on the ground

means that unsteady RANS does indeed predict periodic shedding, however neither RANS nor uRANS are capable of capturing all the properties of the flow around an obstacle in a thin boundary layer in qualitative terms.

Let us consider now the flow behind a cube totally immersed in a boundary layer ($\delta/H = 2.353$). It has turned out that the unsteady calculations detect a very weak periodic motion in the wake for that case. That is why a visible discrepancy between the steady (green line) and unsteady (green square marker) results presented in Figure 4 can be recognized. There are two possible reasons for such effect. The first explanation could be given from the literature data which gives evidence that a thick and turbulent boundary layer tends to suppress the periodic motion. For example, Castro [14] in his experiment has not observed periodicity in the wake of a cube in a thick boundary layer ($\delta/H \approx 6.6$). Some periodicity has been however identified for higher obstacles where parameter δ/H is of the order 1.1. The strong periodicity for a vertical square-cross section cylinder with the width-to-height ratio equal 1/3 and placed in a boundary layer of the thickness of $0.8H$ has been observed by Sakamoto and Haniu [2]. It could be concluded that the flow could be treated as statistically stationary for high δ/H parameter values, hence the unsteady simulation is not necessary and steady calculations alone are sufficient.

The second reason for the lack of periodicity observed in the last case could be attributed to the limitations of uRANS for such type of flows. Fadai-Ghotbi *et al.* [15] have obtained, surprisingly enough, a steady solution for a backward-facing step simulation with a refined mesh. Having conducted a systematical study they have shown the difficulty in reproducing such main characteristics of the flow as the recirculation length, backflow intensity, boundary-layer recovery, especially for a dense mesh and for small expansion ratios. They claim that the spatial numerical oscillations for coarse meshes act as perturbations that are sufficient to excite the natural mode of a shear layer. When the mesh is refined the numerical oscillations decrease and there is no mechanism to excite the shear layer. According to Fadai-Ghotbi *et al.* [15] "the appearance of unsteady solutions can only be a numerical artifact due to the combination of a too coarse mesh and an oscillation-generating scheme". Whatever the reason for the lack of oscillations for a single body, the flow field is much more complex for configurations consisting of obstacles of various height. At first, the obstacles are usually of various height, where the relative inlet boundary layer thickness is of different levels. Additionally, the experimental investigations give evidence that mutual interaction of objects is observed in that case. That is why, an analysis of the flow around two objects in a tandem arrangement will be performed also with the unsteady RANS method in the next chapter.

6. Objects interaction in thick turbulent boundary layer

For multiple bluff bodies arrays, the flow field is more complex than the flow around a single cube by mutual interference. The flow becomes strongly unsteady, both because of the periodicity of vortex shedding and the cyclic oscillatory air movements in between the obstacles.

The flow around configuration of two rectangular tandem arrangement buildings, described by the distance $S/B = 1.5$ and the height ratio $H_1/H_2 = 0.6$, when the objects are aligned in the flow direction with the smaller one located on the upwind side is discussed in this paper (Figure 1b). A strong downwash effect is observed for the relatively small spacing considered here. The big standing vortex which stabilizes the flow in the spacing does not allow the separated shear layers from the lateral sides of windward object to interact in between the obstacles. Additionally, it produces an excessively high velocity at the ground level what is directly correlated with the wall shear stresses distribution on the ground. It is worth mentioning that the downwash effect becomes weaker and the shear layers manage to curl in the gap [16, 17] for larger spacing values not considered in this paper.

The simulation of a configuration with a flow around objects has been done using both the steady and unsteady approaches. Figure 7 gives a comparison of wall shear stresses distributions in the gap between objects. A small discrepancy between steady and unsteady results is recognized at the symmetric line ($y/B = 0$). It is possible as the flow in the spacing is stabilized by the downwash effect. Strong differences between the results are observed at the $y/B = 0.5$ line located along the upstream object edge extension. In this plane, the separated shear layers forming the windward obstacle's lateral sides cannot interact in the gap. The shedding vortices close to the rear side of the upstream object are strong enough (it is shown in Figure 9),

so they influence the solution. It can be observed that the trend of shear stresses distribution is captured well by both numerical results which however overestimate the experimental results (even taking into account the experimental error bars), especially in the central part of the cavity. It could be explained by the well known deficiency of the k-ε model applied for such complex flows.

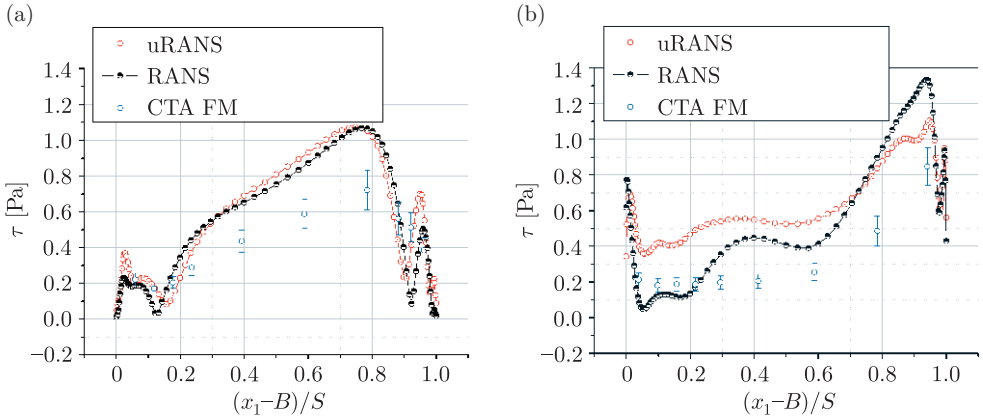

Figure 7. Distribution of wall shear stress for steady and unsteady simulation ($\delta/H_2 = 1.524$, $z/B = 0.0$) in the gap between objects: (a) at the line $y/B = 0$; (b) at the line $y/B = 0.5$

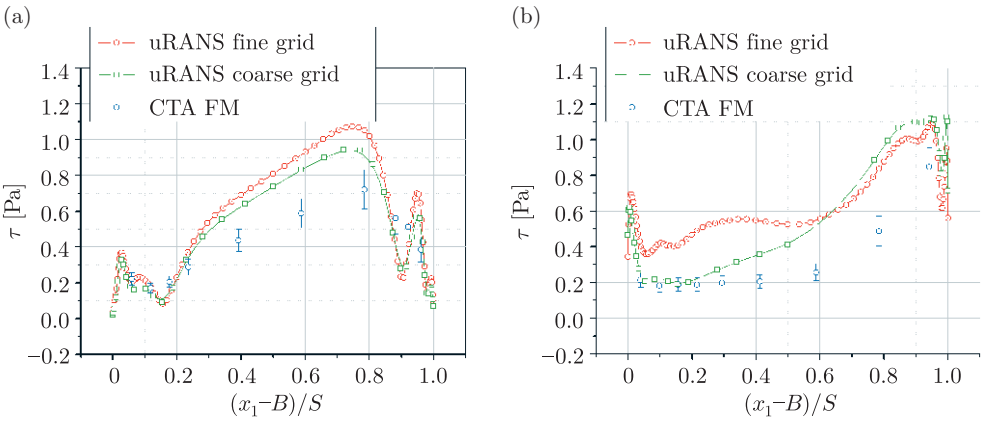

Figure 8. Distribution of wall shear stress for unsteady simulation with fine and coarse grid ($\delta/H_2 = 1.524$, $z/B = 0.0$) in the gap between objects: (a) at the line $y/B = 0$; (b) at the line $y/B = 0.5$

As has been mentioned in the previous chapter, the grid resolution could effect the solution. For this reason, an additional simulation with the coarse grid has been performed. The distribution of wall shear stresses of an unsteady simulation with fine and coarse grids is compared in Figure 8. The discrepancies, at least for the symmetric line, are very slight and concern only the middle part of the space between the objects where the difference between the results from the fine and coarse grids reach only about 15%. At the $y/B = 0.5$ line the discrepancies between the two cases are more clear. The unsteady calculation with the coarse grid provides a better match with

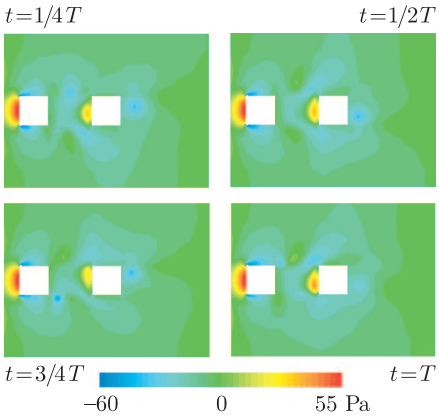

Figure 9. History of the pressure distribution on the ground for tandem arrangement

the experimental data especially in the vicinity of the rear wall of the first obstacle where they directly reflect the distribution of experimental results. It means that the shedding process is reproduced by the simulation on the coarse grid.

An instantaneous solution for two tandem arrangement surface-mounted objects is shown in Figure 9 for selected phases of the shedding cycle. A quality analysis based on the static pressure contours distribution at the ground level indicates the presence of a vortex shedding process for the windward obstacle. The vortices shed from the lateral side of the object are identified with the local island of low static pressure. However, as can be seen, the vortices are pushed out from the cavity by the standing vortex which dominates the flow in this area. This vortex can be recognized by the analysis of instantaneous pictures of the wall shear stresses distribution presented in Figure 10.

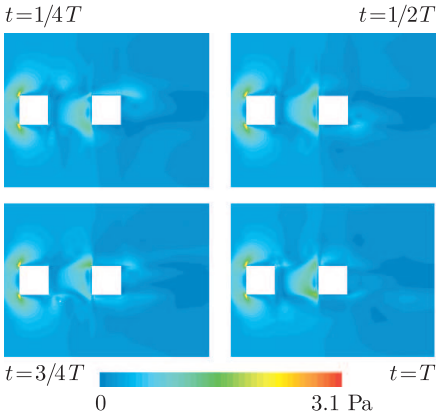

Figure 10. History of the wall shear stresses distribution on the ground for tandem arrangement

For the finer grid case, the shedding process has been damped and this lack of periodicity causes a predominant effect of the standing vortex and an increase in the mean shear stresses seen close to the upstream object at the $y/B = 0.5$ line in particular.

7. Conclusion

A numerical analysis of the flow in the reversed flow region directly behind the body reveals the importance of the inlet boundary layer thickness on the flow structure. It has been shown that the separation length is considerably reduced with an increase in the δ/H parameter. We have demonstrated that the unsteady RANS provides better qualitative agreement with the experiment when the flow is not statistically stationary (low δ/H ratio). However, taking into account the statement of Fadai-Ghotbi *et al.* [15] one should be aware that the unsteady uRANS results must be interpreted with care in terms of temporal variation of forces. Large-scale structures developing in separated shear-layers are not clearly detected for a fine grid.

Acknowledgements

The paper was supported by the State Committee for Scientific Research (KBN) under Grant No. 4T07F00329.

References

[1] Martinuzzi R J and Tropea C 1993 *J. Fluid Eng.* **115** 85
[2] Sakamoto H and Haniu H 1988 *J. Wind Eng. and Ind. Aerodyn.* **31** 41
[3] Schofield W H and Logan E 1990 *J. Fluid Eng.* **112** 376
[4] Martinuzzi R J and Havel B 2000 *J. Fluid Eng.* **122** 24
[5] Ferreira A D, Sousa A C M and Viegas D X 2002 *J. Wind Eng. and Ind. Aerodyn.* **90** 305
[6] Richards P J, Mallinson G D, McMillan D and Li Y F 2002 *Wind and Structures* **5** (2–4) 151
[7] Franke J, Hirsch C, Jensen A G, Wisse J A and Wright N G 2004 *Recommendation on the Use of CFD in Predicting Pedestrian Wind Environment*, *COST C14*
[8] Huptas M 2006 *Preliminary Investigations on the Role of Inlet Boundary Conditions in Numerical Analysis of the Flow in Built-up Areas*, Internal Report, **IMC-27/2006/2** (in Polish)
[9] Richards P J and Hoxey R P 1993 *J. Wind Eng. and Ind. Aerodyn.* **46-47** 145
[10] Hu C-H and Wang F 2005 *Building and Environment* **40** 617
[11] Hunt J C R, Abell C J, Peterka J A and Woo H 1978 *J. Fluid Mech.* **86** 179
[12] Castro I P and Robins A G 1977 *J. Fluid Mech.* **79** 307
[13] Iaccarino G, Ooi A, Durbin P A and Behnia M 2003 *J. Heat and Fluid Flow* **24** 147
[14] Castro I P 1981 *J. Wind Eng. and Ind. Aerodyn.* **7** 253
[15] Fadai-Ghotbi A, Manceau R and Borée J 2008 *Revisiting URANS Computations of the Backward-facing Step Flow Using Second Moment Closures. Influence of the Numerics*, "Flow, Turbulence and Combustion", Springer Netherlands, ISSN 1386-6184 (printed), 1573-1987 (online)
[16] Huptas M 2008 *Steady Simulation of the Flow Field Around Two Objects Configuration of Varying Geometrical Parameters*, Internal Report, **IMC-3/2008/1** (in Polish)
[17] Huptas M 2008 *Unsteady Simulation of the Flow Field Around Two Objects Configuration of Varying Geometrical Parameters*, Internal Report, **IMC-3/2008/2** (in Polish)